J. Microbiol. Biotechnol. (2013), 23(7), 923–931
http://dx.doi.org/10.4014/jmb.1304.04057

jmb

Metabolomic Response of *Chlamydomonas reinhardtii* to the Inhibition of Target of Rapamycin (TOR) by Rapamycin S

Do Yup Lee[1]* and Oliver Fiehn[2]*

[1]*Department of Advanced Fermentation Fusion Science and Technology, Kookmin University, Seoul 136-702, Republic of Korea*
[2]*Genome Center, University of California, Davis, CA 95616, USA*

Received: April 23, 2013
Revised: May 1, 2013
Accepted: May 2, 2013

First published online
June 3, 2013

**Corresponding authors*
O.F.
Phone: +1-530-754-8258;
Fax: +1-530-754-9658;
E-mail: ofiehn@ucdavis.edu
D.Y.L.
Phone: +82-2-910-5733;
Fax: +82-2-910-5733;
E-mail: rome73@kookmin.ac.kr

Supplementary data for this paper are available on-line only at http://jmb.or.kr.

pISSN 1017-7825, eISSN 1738-8872

Rapamycin, known as an inhibitor of Target of Rapamycin (TOR), is an immunosuppressant drug used to prevent rejection in organ transplantation. Despite the close association of the TOR signaling cascade with various scopes of metabolism, it has not yet been thoroughly investigated at the metabolome level. In our current study, we applied mass spectrometric analysis for profiling primary metabolism in order to capture the responsive dynamics of the *Chlamydomonas* metabolome to the inhibition of TOR by rapamycin. Accordingly, we identified the impact of the rapamycin treatment at the level of metabolomic phenotypes that were clearly distinguished by multivariate statistical analysis. Pathway analysis pinpointed that inactivation of the TCA cycle was accompanied by the inhibition of cellular growth. Relative to the constant suppression of the TCA cycle, most amino acids were significantly increased in a time-dependent manner by longer exposure to rapamycin treatment, after an initial down-regulation at the early stage of exposure. Finally, we explored the isolation of the responsive metabolic factors into the rapamycin treatment and the culture duration, respectively.

Keywords: Metabolomics, mass spectrometry, *Chlamydomonas reinhardtii*, target of rapamycin

Introduction

Rapamycin, known as sirolimus, is an immunosuppressant drug used to prevent rejection in organ transplantation [26], and is produced by the bacterial species *Streptomyces hygroscopicus* [32]. Rapamycin binds the cytosolic protein FK-binding protein 12 (FKBP12), inhibits downstream signaling from the target of rapamycin (TOR) proteins [10], and eventually hinders cellular growth and proliferation, making this molecule an important potential target for various diseases. The evolutionarily conserved protein kinase (PK) TOR, is ubiquitously present in organisms, from yeast to plants and humans. Yeast genetics screened the identification of TOR as one mediator of the toxic effect of rapamycin in yeast [13], followed by the discovery of the mechanistic TOR (mTOR) as the physical target of rapamycin in mammalian cells [3]. TOR in yeasts and mammals is known to integrate diverse external and internal signals, and regulates cellular metabolism and growth by keeping a persistent level of nutrient supply, ribosome biogenesis, and mRNA translation [33]. Several reports have also shown the molecular and physiological functionalities of TOR in the plant kingdom, notably for *Arabidopsis* [12, 20, 22]. However the growth of *Arabidopsis thaliana* and other plants such as *Oryza sativa*, *Nicotiana tabacum*, or *Brassica napus* is not sensitive to rapamycin [22], probably due to a generic incapability of the plant FKBP12 to bind rapamycin, which may hinder the progress of the research on TOR signaling in photosynthetic organisms. Recently, it has been noted that TOR inhibition by rapamycin inhibits the growth of the photosynthetic unicellular alga *Chlamydomonas reinhardtii* [22] and following studies successfully identified the molecular evidence and cellular physiology in *C. reinhardtii* [5, 6, 24].

Considering these results, we carried out an analysis of rapamycin-induced effects on *Chlamydomonas* cells with a

focus on primary metabolism, which has so far only been investigated in *Arabidopsis* [4], despite the tight linkage between the TOR signaling pathway and a range of central metabolism. In order to link the mTOR-mediated control of biomass growth in *Chlamydomonas* to changes in primary metabolism, we present here gas chromatography/time-of-flight mass-spectrometry (GC/TOF MS)-based metabolite profiling [8, 9]. We show that the inhibition of TOR by rapamycin induces a massive impact on the primary metabolism in *Chlamydomonas*, yielding very distinct metabolic phenotypes in a time-dependent manner.

Materials and Methods

Cell Culture

Chlamydomonas reinhardtii strain CC125 was used for the whole study. The strain was cultured in TAP medium [11] at 23ºC under constant illumination with cool-white fluorescent bulbs at a fluence rate of 70 µmol m^{-2} s^{-1}. After 48 h, a starter culture was inoculated at a starting density of 5.0×10^6 cells/ml in 25 ml of Tris-buffered medium under two different treatments (rapamycin treatment and the control). Rapamycin was added to give final concentrations of 500 nM from a 1 mg/ml stock in 90% ethanol-10% Tween20 [5] whereas mock-treated control groups were provided blank vehicle without rapamycin. For measuring cell densities, we selected 4 time points (3, 10, 24, and 48 h), which represent the lag, early exponential, early stationary, and late stationary phases, respectively. For harvesting cells for metabolite profiling, we chose two time points (24 and 48 h), in which 0.5 and 1 ml of control and treated cell suspensions were rapidly mixed into 0.5 and 1 ml of −70ºC cold quenching solutions composed of 70% methanol in water, respectively. Following a quick centrifugation (2 min), pellets were lyophilized and stored at −80ºC until further analysis.

Extraction Method and Sample Preparation of Metabolites

For metabolites profiling, procedures followed the protocol we had previously reported [17, 18]. Briefly, lyophilized cells were disrupted using a single 5 mm i.d. steel ball, followed by the addition of 0.75 ml of an extraction solvent of methanol:chloroform: water (5:2:2) and vortexing. After a 2 min centrifugation at 16,100 ×*g*, 0.70 ml extracts were collected and concentrated to dryness for further analysis. Then 5 µl of a solution of 20 mg/ml of 98% pure methoxyamine hydrochloride (CAS No. 593-56-6; Sigma, USA) in pyridine (silylation grade; Pierce, USA) was added and shaken at 30ºC for 90 min to protect aldehyde and ketone groups. Then 45 µl of MSTFA with 1% TMCS (1 ml bottles; Pierce) was added for trimethylsilylation of acidic protons and shaken at 37ºC for 30 min with 1 µl of internal retention index markers composed of fatty acid methyl esters of C8, C9, C10, C12, C14, C16, C18, C20, C22, C24, C26, C28, and C30 linear chain lengths.

Mass Spectrometry Analysis

The resulting sample was managed using a Gerstel automatic liner exchange system with multipurpose sample MPS2 dual rail controlled by the Maestro software, to inject a 0.5 µl sample to a Gerstel CIS cold injection system (Gerstel, Germany). The injector was operated in splitless mode, and the split vent was opened after 25 sec. Samples were injected into the 50ºC injector port, which was ramped to 250ºC at 12ºC/min and held for 3 min. For chromatographic separation, the Agilent 6890 gas chromatograph (Agilent, USA) was used, which was equipped with a 30 m long, 0.25 mm i.d. Rtx5Sil-MS column (Restek (USA), 0.25 mm of a 5% diphenyl film, and additional 10 m integrated guard column). Mass spectrometry was performed by a Leco Pegasus III time-of-flight mass spectrometer (Leco, USA). Result files were preprocessed directly after data acquisition and stored as ChromaTOF-specific *.peg files, as generic *.txt result files, and additionally as generic ANDI MS *.cdf files. For more details see Lee and Fiehn [18] and Kind *et al.* [15]. Raw data were normalized by factors that were calculated from the sum of intensities of the identified compound [14, 17]. Data were further log-transformed and normalized using Pareto normalization [23] for clustering analysis and two-way ANOVA.

Statistics

Statistical analyses were performed using the Statistica software ver. 7.1 (StatSoft, USA). Univariate statistics for multiple study design classes was performed by the Student t-test, one-way ANOVA, and two-way ANOVA. F-Statistics and p-values were calculated for all metabolites. Data distributions were displayed by box-whisker plots, giving the arithmetic mean value for each category, the standard error as box and whiskers for 1.96 times the category standard error to indicate the 95% confidence intervals, assuming normal distributions. Multivariate statistics was performed by unsupervised principal component analysis (PCA) by entering metabolite values without study class assignments. In addition, a three-dimensional scatterplot was constructed by three vectors ordered according to the degree of variance in metabolite abundance [17].

Results and Discussion

Inhibitory Effect of Rapamycin on *Chlamydomonas* Cellular Growth

Up to 10 h of culture (lag to early exponential phases) after 500 nM of rapamycin treatment, no statistical difference was observed in cellular growth between control and rapamycin-treated cells. This observation was consistent with the previous report, where incomplete arrest of the *Chlamydomonas* growth was observed, unlike yeast [1, 5, 24]. After 24 h, at which cells transitioned through the late exponential phase to the early stationary phase, the cellular

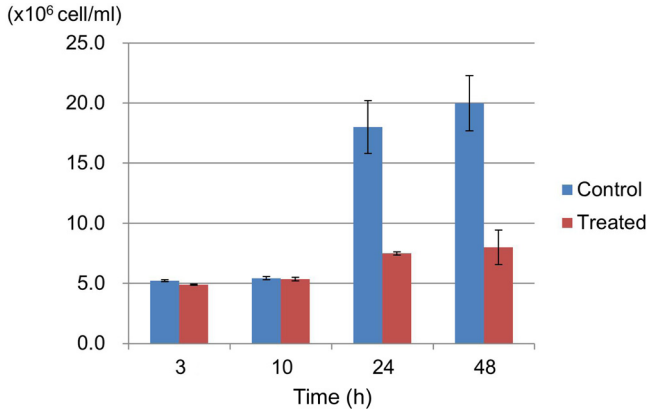

Fig. 1. Cell number density of the control and the treated samples (n = 6 for each) along four time points.

growth was significantly suppressed by the rapamycin treatment, which was followed by the complete inhibition of the cell growth of *Chlamydomonas* at 48 h (late stationary phase) exposure to the rapamycin treatment (Fig. 1). Since we observed the distinctiveness in cellular physiology after the cells entered early stationary phase at 24 h, two time points (24 and 48 h) were selected for metabolomic investigation regarding primary metabolism in response to TOR inhibition by rapamycin treatment, using gas chromatography-coupled time-of-flight mass spectrometry.

Phenotyping the Metabolic Response of *Chlamydomonas* to Rapamycin Treatment

We performed metabolite profiling of *Chlamydomonas* samples obtained from two treatments (control and rapamycin-treated cells) along two time points (24 and 48 h) in order to resolve the time-dependent dynamics of the responsive metabolome. A total of 136 metabolic signals were structurally identified by GC-MS using the BinBase algorithm, with a 50% occurrence in at least one class of samples, which systematically excluded known artifacts such as phthalates or polysiloxanes. The endogenous metabolites were amines, amino acids, carbohydrates, fatty acids, and organic acids that fairly cover the primary metabolism of *Chlamydomonas* cells.

First, multivariate analysis demonstrated that the principal components differentiating the metabolic profiles were linked to the time-dependent rapamycin treatment. By using unsupervised principal component analysis (PCA), vector 1 (24.3% total explained variance) mostly separated all clusters, including different treatment and time points (Fig. 2A). When vector 2 (13.0%) and vector 3 (11.0%) were applied to the sample scatterplot, the distinctiveness was even clearer among the four different groups (Fig. 2B). The results imply that the inhibition of TOR by rapamycin affects a range of the primary metabolism in which the integrative metabolomic phenotype was clearly discriminated.

Rapamycin Treatment Induces Differential Regulation of Metabolism

Univariate analysis of the variance was applied to interrogate compositional changes in metabolites associated with rapamycin treatment. In the early stage (24 h), a total of 51 metabolites were significantly changed with rapamycin treatment, in which 17 compounds were increased while 34 chemicals were down-regulated. Among the increased, three

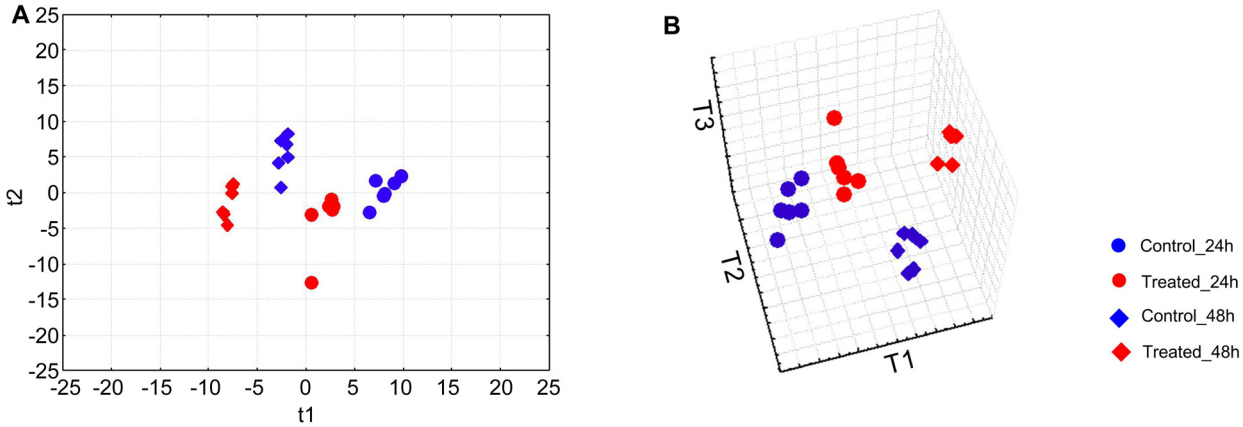

Fig. 2. Principal component analysis of metabolomic profiles of 136 metabolites of *C. reinhardtii* cultures grown under normal conditions and rapamycin treatments, followed for 24 and 48 h after inoculation.

(**A**) T1 indicates discriminating vector 1 that explained the largest degree of variation in the dataset. Likewise, T2 indicates principal component 2, and with combination T3, the three-dimensional scatterplot of samples is constructed.

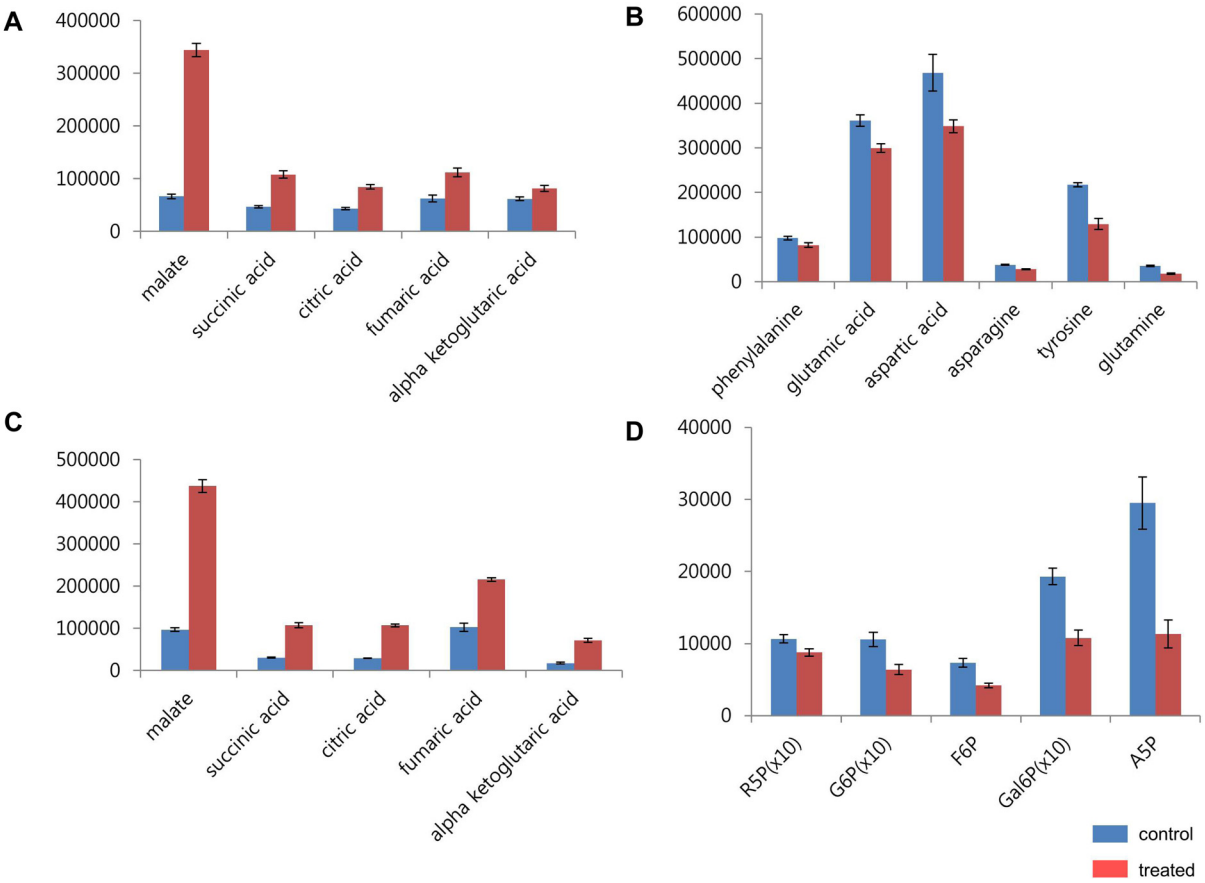

Fig. 3. Effect of TOR inhibition by rapamycin treatment on the metabolites contents.
Metabolites showing significant changes by rapamycin treatment were calculated by the Student t-test; units: normalized peak heights. Bars indicate standard errors. (**A**) and (**B**) indicate the list of significantly up-regulated and down-regulated metabolites, respectively, at 24 h culture by rapamycin treatment. (**C**) and (**D**) present the significantly up-regulated and down-regulated metabolites, respectively, at 48 h culture by rapamycin treatment. R5P, ribose-5-phosphate; G6P, glucose-6-phosphate; F6P, fructose-6-phosphate; Gal6P, galactose-6-phosphate; A5P, adenosine-5-phosphate.

TCA cycle intermediates, malate, succinate, and citrate, showed the highest statistical significances ($p < 6.6\times10^{-6}$) (Fig. 3A). Furthermore, pathway analysis indicated that the TCA cycle was the most prominent among the up-regulated metabolisms (FDR = 1.2×10^{-4}), using the hypergeometric test as overrepresentation analysis [34]. The altered activity of the TCA cycle was accompanied by the simultaneous down-regulation of many amino acids such as phenylalanine, glutamic acid, aspartic acid, asparagine, tyrosine, and glutamine (Fig. 3B), all of which showed the highest involvement in protein biosynthesis (translation, FDR = 1.0×10^{-4}) and nitrogen metabolism (FDR = 1.8×10^{-3}) by the hypergeometric test of pathway analysis.

Longer exposure to rapamycin (48 h) did not lead to a higher number of differentially regulated metabolites, indicating that *Chlamydomonas* cells appear to be more resistant to rapamycin treatment than other single cellular microorganisms such as yeast [17]. Thirty-two compounds showed significant increase in the cellular contents associated with the rapamycin treatment. Similar to the 24 h time period, the TCA cycle intermediates malate, succinate, and α-ketoglutaric acid showed the most dramatic changes in comparison with those of the control samples. The concomitant up-regulation of these metabolites can be interpreted as the accumulation driven by lesser use of the TCA cycle intermediates as carbon backbones for the biosynthetic process, which accordingly led to cellular growth inhibition (Figs. 3A and 3C). It has been denoted by the metabolic profiling study of *Arabidopsis* that the inhibition of TOR (by conditional down-regulation of the AtTOR gene) led to a

prominent effect on the TCA cycle flux and the redox state of the cell, which was metabolically characterized by the accumulation of TCA cycle intermediates such as citrate, α-ketoglutarate, succinate, fumarate, and malate [4].

Of particular interest, amino acids presented the dynamic alteration in a time-dependent manner. In addition to the up-regulation of amino acids driven by increased influx *via* protein degradation, as observed in *Arabidopsis* metabolism [4], we could capture the transient reduction of amino acids at the early stage (24 h). The temporal down-regulation of the amino acids can be linked to the increased energy- and nutrient-providing catabolic activities that accompanied the inactivation of the TCA cycle, and precede nutrient recycling processes such as senescence or autophagy.

Additionally, we noted a consistent down-regulation of various key intermediates of primary metabolism in glycolysis (glucose-6-phosphate, fructose-6-phosphate, galactose-6-phosphate), pentose phosphate pathway (ribose-5-phosphate), and nucleotides (guanine, adenosine-5-monophosphate) (Fig. 3D). It has been reported that phosphate homeostasis is altered by the disturbance of TOR signaling with rapamycin treatment [31], which was biochemically phenotyped by simultaneous depletion of endogenous phosphorylated metabolites in the current study. The reduced levels of the phosphorylated carbohydrates can also be linked to the increased activity of starch biosynthesis that coincided with the increased levels of a range of hexose and phosphorylated carbohydrates [2]. The concomitant suppression of phosphorylated carbohydrates was also reported in inducible artificial microRNA lines of *Arabidopsis* for the conditional down-regulation of the AtTOR gene [4].

Co-Regulatory Structures of Metabolomic Dynamics to Rapamycin Treatment

In addition to univariate and multivariate analyses (PCA) of the responsive metabolism, we applied hierarchical clustering analysis (HCA) using Spearman rank correlation [29] and average linkage methods [7]. The analysis, beyond the capabilities of univariate and multivariate analyses, can simultaneously explore sample- and variable-wise statistical linkages. The statistics resulted in clustering of biologically and biochemically related group of samples, and evaluates the chemical classification of the treatment and temporal metabolic signature derived from the co-regulated expression pattern. Like the PCA results, the HCA revealed a high correlation of each biological group, with significant difference between the control and the treated samples (Fig. 4). In order to statistically divide the entries of correlated metabolites, we used the Self Organizing Tree Algorithm

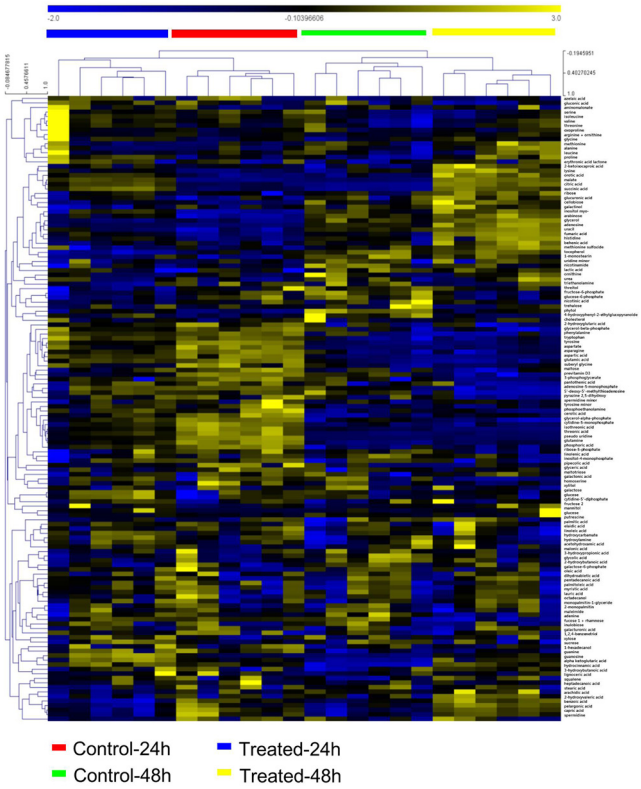

Fig. 4. Hierarchical clustering analysis.
Clustering analysis was performed across the metabolites and samples using Spearman rank correlation and average linkage methods. Each column and each row represent a *Chlamydomonas* sample and an individual metabolite, respectively.

(SOTA), which allows for constructing a binary tree (dendrogram) where the terminal nodes are the resulting clusters [19, 30]. In this way, four representative clusters were obtained (Fig. 5).

In cluster 1, co-regulated metabolites showed expression patterns in which the constant up-regulation of metabolites was specifically identified in treated groups compared with those of control groups at both the 24 and 48 h time points (Fig. 5A). The metabolites included TCA cycle intermediates such as succinic acid, malate, citric acid, and α-ketoglutaric acid. The co-regulated module was also observed in the biochemical relevance that consists of such amino acids as proline, oxoproline, lysine, glycine, valine, and threonine, which is a typical metabolic phenotype under nitrogen depletion that is mimicked by the inhibition of TOR [4]. Of particular interest were the increased levels of proline and oxoproline that corresponded to the previously reported hyperphosphorylation of the activator of the proline utilization pathway [27].

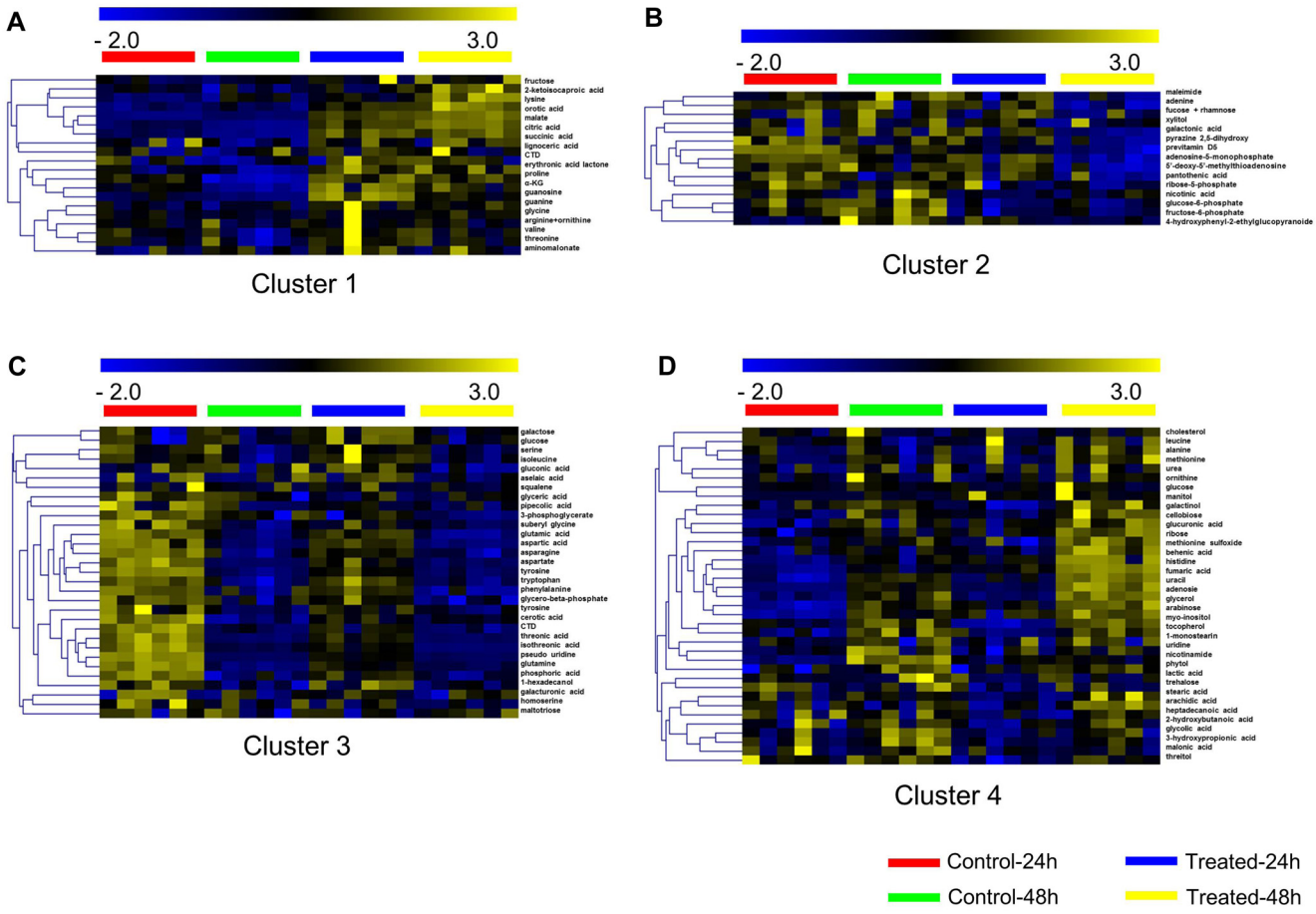

Fig. 5. Self Organizing Tree Algorithm (SOTA) map, applied for clustering co-regulated metabolites into definite groups.
Plots A, B, C, and D represent four clusters, out of a total of 5 recognized clusters obtained by this analysis, containing the assigned metabolites.

We observed another type of treatment-dependent co-regulation (cluster 2) whose pattern was opposite to cluster 1, as the compounds in this group were significantly reduced by the rapamycin treatment at both time points (Fig. 5B). In particular, intermediates of purine metabolism were included as were the metabolites associated with zeatin biosynthesis, which is involved in various processes of growth and development in plants. In comparison, clusters 3 and 4 were indicators of the time-dependent co-regulation, in that the metabolite expression was dominated mainly by culture duration but also partially affected by the rapamycin treatment. The compounds of cluster 3 were co-up-regulated along with an increase of culture duration, and the level of the induction was higher in the treated group compared with the control (Fig. 5C). Various types of lipid molecules are included in this cluster, such as the long-chain saturated fatty acids heptadecanoic acid (C17:0), stearic acid (C18:0), eicosanoic acid (C:20), docosanoic acid (C22:0), as well as carboxylic acids (3-hydroxypropionic acid and 2-hydroxybutanoic acid), cholesterol, and 1-monostearin. Along with the time-dependent co-up-regulation in both control and treated samples, long-chain fatty acids (LCFA) such as eicosanoic acid (C20:0), docosanoic acid (C22:0), and tetracosanoic acid (C24:0) were significantly accumulated by TOR inhibition at the late stage (48 h). The alteration of lipid metabolism was featured in *Arabidopsis* metabolism, in which various types of triacylglycerides, a major storage form for highly reduced carbon and energy, were significantly accumulated [4]. The co-regulatory matrices were extended to such nitrogen-containing chemicals as ornithine, methionine sulfoxide, methionine, leucine, histidine, alanine, adenosine, and the intermediates of uridine metabolism.

Likewise, cluster 4 was characterized by a time-dependent metabolic response (Fig. 5D). The highest level of expression was detected in the control of the 24 h culture that decreased in the contents following the time-course. A

similar pattern was observed in the rapamycin-treated group but with a relatively small reduction. This cluster consisted of the largest number of amino acids, among which the highest enrichment was observed in gly-ser-thr metabolism. The expression pattern of the cluster implied the immediate response of the amino acid metabolism to rapamycin-inhibited TOR at the early stage that was equilibrated as being transitioned to the stationary phase in which nitrogen resources were depleted in both conditions (the rapamycin-treated and the control samples).

Resolving the Contribution of Metabolic Features to the Treatment, Culture Duration, and Interaction

To resolve the significant effect of more than one variable (treatment, time, and treatment × time) on the *Chlamydomonas* metabolism, we used two-way analysis of variance (ANOVA). The two-way ANOVA test is an extension of the one-way ANOVA test that analyzes the effect of different categorical independent variables on one dependent variable, in this case, metabolite. Thus, the two-way ANOVA not only determines the main effect of the contributions of each independent variable but also distinguishes if there is a significant interaction between the independent variables. Indeed, the analysis resolved the rapamycin treatment-dependent and culture duration-dependent influences, respectively. As summarized in Fig. 6A, a total of 79 metabolites were significant effectors that influence the metabolic responses. Among them, exclusive factors for rapamycin treatments were glucose-6-phosphate (Fig. 6B), galactose-6-phosphate, and fructose-6-phosphate (Supplementary Fig. S1). Those metabolites showed differential down-regulation of metabolite contents by rapamycin treatment with a minimal level of differences between both time points. In comparison, rapamycin treatment induced the

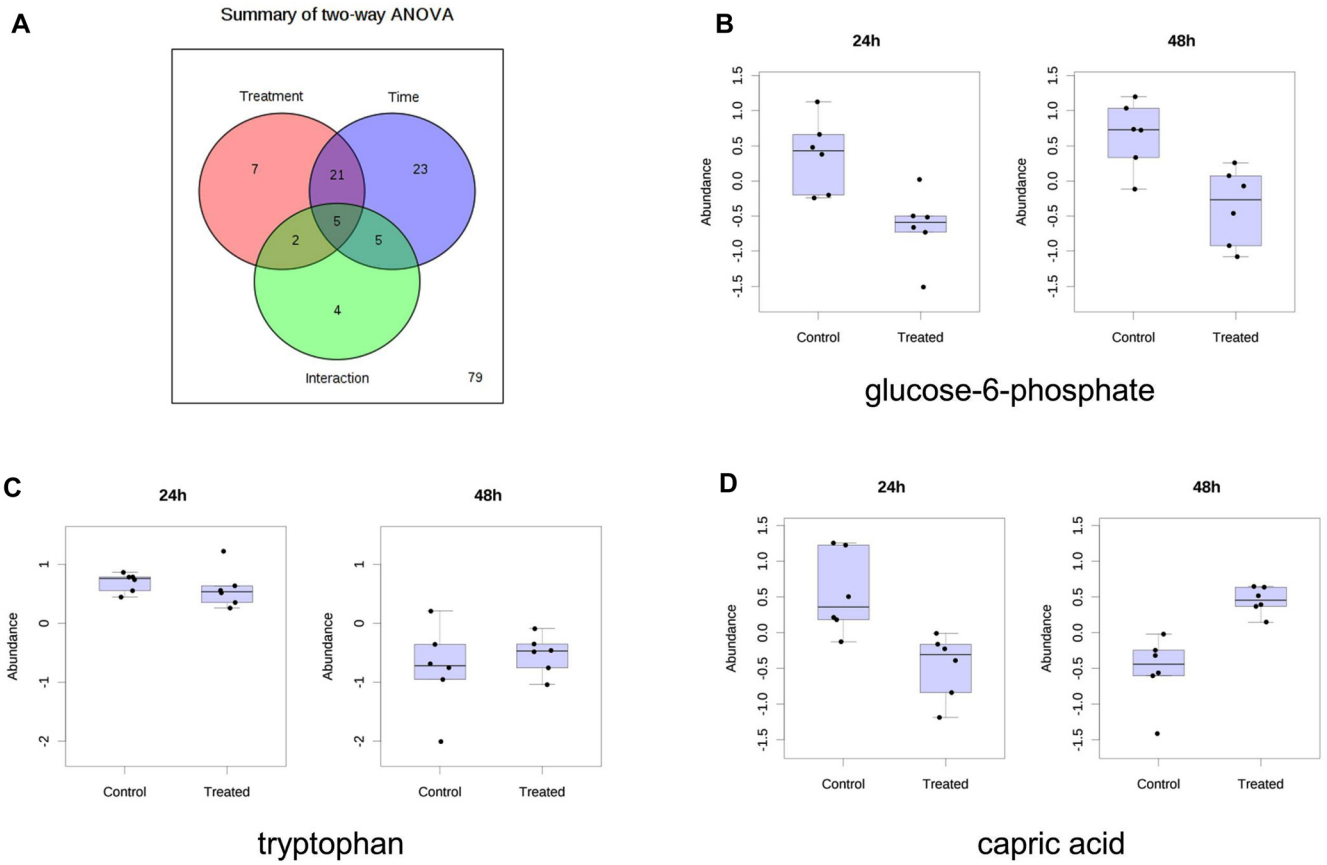

Fig. 6. Two-way ANOVA results.

(**A**) The summary of the two-way ANOVA. Box-and-Whisker plots arranged horizontally on (**B**) glucose-6-phosphate, (**C**) tryptophan, and (**D**) capric acid. Units are normalized abundances and the line in the middle of box is the median. The box illustrates the lower and upper quartile of values, respectively, and each datum point is plotted as a dot.

increased synthesis of the amino acid proline at both time points, implying the specific activation of the proline pathway by rapamycin-induced TOR inhibition in *Chlamydomonas*.

Additionally, we investigated the temporal effects on metabolism that were independent of the rapamycin treatment responses. We selected metabolites by filtering the data with the smallest *p*-value for time factor and the largest *p*-value for treatment component. This captured a trend in which the computed metabolites showed dominant time-dependent changes but minimal differences due to rapamycin treatment. Among the metabolites are such amino acids as tryptophan (Fig. 6C), aspartic acids, asparagine, and phenylalanine (Supplementary Fig. S2).

The two-way ANOVA test also demonstrated that some compounds differed both by treatment and temporal dependence (Fig. 6D). In contrast to the factors that were only found for either treatment or time, such co-dependence represents the dynamics of metabolic regulation in cells with opposite regulation of metabolite contents at early and late responses to rapamycin. For example, nonanoic acid was significantly down-regulated in the treated group, but the level was dramatically increased at the 48 h time point. The same types of regulation of metabolite levels were monitored in another medium-chain fatty acid, capric acid, and in benzoic acid (Supplementary Fig. S3). Capric acid may function as an antioxidant [28] induced by the rapamycin-enhanced oxidative stress response [16, 21]. As an aromatic carboxylic acid, benzoic acid and its derivatives are known to be important structural elements, playing many valuable roles in plant growth regulators and defensive compounds [25]. Collectively, the findings in the present study indicate that molecular features provides, the unique metabolomic phenotype, which can differentiate the metabolic disturbance by TOR inhibition as well as culture duration of the *Chlamydomonas* cells, by applying the multivariate statistics. Statistical analysis captures the concerted metabolic modulation that can in general be characterized by four chemical groups (amino acids, fatty acids, phosphorylated carbohydrates, and the intermediates of the TCA cycle). In particularly, amino acids demonstrate the diverse expression pattern that will aid in specifying the role and mechanism of individual compounds in the response to the rapamycin treatment. Finally, we were able to dissemble the metabolic influence by the TOR inhibition into the individual effectors on the responsive metabolism of *Chlamydomonas*. This study presents the first approach to identify the metabolome-scale responses to TOR inhibition by rapamycin treatment in microorganisms, which will help to unravel the complicated involvement of the TOR signaling cascade for future researches.

Acknowledgments

This work was partly funded by the National Science Foundation grant MCB 1139644 (USA) and by the new faculty research Program (J 2013-0048) of Kookmin University in Korea.

References

1. Barbet N, Schneider U, Helliwell S, Stansfield I, Tuite M, Hall M. 1996. TOR controls translation initiation and early G1 progression in yeast. *Molec. Biol. Cell* **7:** 25.
2. Benkeblia N, Shinano T, Osaki M. 2007. Metabolite profiling and assessment of metabolome compartmentation of soybean leaves using non-aqueous fractionation and GC-MS analysis. *Metabolomics* **3:** 297-305.
3. Brown EJ, Albers MW, Shin TB, Ichikawa K, Keith CT, Lane WS, *et al*. 1994. A mammalian protein targeted by G1-arresting rapamycin-receptor complex. *Nature* **369:** 756-758.
4. Caldana C, Li Y, Leisse A, Zhang Y, Bartholomaeus L, Fernie AR, *et al*. 2013. Systemic analysis of inducible target of rapamycin mutants reveal a general metabolic switch controlling growth in *Arabidopsis thaliana*. *Plant J*. **73:** 897-909.
5. Crespo JL, Díaz-Troya S, Florencio FJ. 2005. Inhibition of target of rapamycin signaling by rapamycin in the unicellular green alga *Chlamydomonas reinhardtii*. *Plant Physiol.* **139:** 1736-1749.
6. Díaz-Troya S, Florencio FJ, Crespo JL. 2008. Target of rapamycin and LST8 proteins associate with membranes from the endoplasmic reticulum in the unicellular green alga *Chlamydomonas reinhardtii*. *Eukaryotic Cell* **7:** 212-222.
7. Eisen MB, Spellman PT, Brown PO, Botstein D. 1998. Cluster analysis and display of genome-wide expression patterns. *Proc. Natl. Acad. Sci. USA* **95:** 14863-14868.
8. Fiehn O, Kopka J, Dörmann P, Altmann T, Trethewey RN, Willmitzer L. 2000. Metabolite profiling for plant functional genomics. *Nature Biotechnol.* **18:** 1157-1161.
9. Goodacre R, Vaidyanathan S, Dunn WB, Harrigan GG, Kell DB. 2004. Metabolomics by numbers: Acquiring and understanding global metabolite data. *Trends Biotechnol.* **22:** 245-252.
10. Guba M, von Breitenbuch P, Steinbauer M, Koehl G, Flegel S, Hornung M, *et al.* 2002. Rapamycin inhibits primary and metastatic tumor growth by antiangiogenesis: Involvement of vascular endothelial growth factor. *Nature Med.* **8:** 128-135.
11. Harris EH, Stern DB, Witman G. 1989. *The Chlamydomonas Sourcebook*. Cambridge University Press, UK.
12. He Z, Li L, Luan S. 2004. Immunophilins and parvulins. Superfamily of peptidyl prolyl isomerases in *Arabidopsis*. *Plant Physiol.* **134:** 1248-1267.

13. Heitman J, Movva NR, Hall MN. 1991. Targets for cell cycle arrest by the immunosuppressant rapamycin in yeast. *Science* **253:** 905-909.
14. Hutschenreuther A, Kiontke A, Birkenmeier G, Birkemeyer C. 2012. Comparison of extraction conditions and normalization approaches for cellular metabolomics of adherent growing cells with GC-MS. *Anal. Methods* **4:** 1953-1963.
15. Kind T, Wohlgemuth G, Lee DY, Lu Y, Palazoglu M, Shahbaz S, *et al*. 2009. FiehnLib: Mass spectral and retention index libraries for metabolomics based on quadrupole and time-of-flight gas chromatography/mass spectrometry. *Anal. Chem.* **81:** 10038-10048.
16. Kofman AE, McGraw MR, Payne CJ. 2012. Rapamycin increases oxidative stress response gene expression in adult stem cells. *Aging (Albany NY)* **4:** 279.
17. Lee D, Park J, Barupal D, Fiehn O. 2012. System response of metabolic networks in *Chlamydomonas reinhardtii* to total available ammonium. *Mol. Cell. Proteomics* **11:** 973-988.
18. Lee DY, Fiehn O. 2008. High quality metabolomic data for *Chlamydomonas reinhardtii*. *Plant Methods* **4:** 7.
19. Luo F, Khan L, Bastani F, Yen I-L, Zhou J. 2004. A dynamically growing self-organizing tree (DGSOT) for hierarchical clustering gene expression profiles. *Bioinformatics* **20:** 2605-2617.
20. Mahfouz MM, Kim S, Delauney AJ, Verma DPS. 2006. *Arabidopsis* target of rapamycin interacts with raptor, which regulates the activity of S6 kinase in response to osmotic stress signals. *Plant Cell* **18:** 477-490.
21. Marobbio CM, Pisano I, Porcelli V, Lasorsa FM, Palmieri L. 2012. Rapamycin reduces oxidative stress in frataxin-deficient yeast cells. *Mitochondrion* **12:** 156-161.
22. Menand B, Desnos T, Nussaume L, Berger F, Bouchez D, Meyer C, *et al*. 2002. Expression and disruption of the *Arabidopsis* TOR (target of rapamycin) gene. *Proc. Natl. Acad. Sci. USA* **99:** 6422-6427.
23. Messac A, Ismail-Yahaya A, Mattson CA. 2003. The normalized normal constraint method for generating the Pareto frontier. *Struct. Multidiscip. Opt.* **25:** 86-98.
24. Pérez-Pérez ME, Florencio FJ, Crespo JL. 2010. Inhibition of target of rapamycin signaling and stress activate autophagy in *Chlamydomonas reinhardtii*. *Plant Physiol.* **152:** 1874-1888.
25. Qualley AV, Widhalm JR, Adebesin F, Kish CM, Dudareva N. 2012. Completion of the core β-oxidative pathway of benzoic acid biosynthesis in plants. *Proc. Natl. Acad. Sci. USA* **109:** 16383-16388.
26. Saunders RN, Metcalfe MS, Nicholson ML. 2001. Rapamycin in transplantation: A review of the evidence. *Kidney Int.* **59:** 3-16.
27. Saxena D, Kannan K, Brandriss MC. 2003. Rapamycin treatment results in GATA factor-independent hyperphosphorylation of the proline utilization pathway activator in *Saccharomyces cerevisiae*. *Eukaryotic Cell* **2:** 552-559.
28. Sengupta A, Ghosh M. 2012. Comparison of native and capric acid-enriched mustard oil effects on oxidative stress and antioxidant protection in rats. *Br. J. Nutr.* **107:** 845.
29. Sturn A, Quackenbush J, Trajanoski Z. 2002. Genesis: Cluster analysis of microarray data. *Bioinformatics* **18:** 207-208.
30. Törönen P, Kolehmainen M, Wong G, Castrén E. 1999. Analysis of gene expression data using self-organizing maps. *FEBS Lett.* **451:** 142-146.
31. Tataranni T, Biondi G, Cariello M, Mangino M, Colucci G, Rutigliano M, *et al.* 2011. Rapamycin-induced hypophosphatemia and insulin resistance are associated with mTORC2 activation and klotho expression. *Am. J. Transplant.* **11:** 1656-1664.
32. Vezina C, Kudelski A, Sehgal S. 1975. Rapamycin (AY-22,989), a new antifungal antibiotic. I. Taxonomy of the producing streptomycete and isolation of the active principle. *J. Antibiotics* **28:** 721.
33. Wullschleger S, Loewith R, Hall MN. 2006. TOR signaling in growth and metabolism. *Cell* **124:** 471-484.
34. Xia J, Mandal R, Sinelnikov IV, Broadhurst D, Wishart DS. 2012. MetaboAnalyst 2.0 – a comprehensive server for metabolomic data analysis. *Nucleic Acids Res.* **40:** W127-W133.